PLOS | **SUBMISSION**

Ultradian Oscillation of Growth Reveals Regulatory Mechanism in the Straightening Movement of Wheat Coleoptile

Renaud Bastien[1*], Stéphane Douady[2], Bruno Moulia[3]

1 Department of Collective Behaviour, Max Planck Institute for Ornithology and Department of Biology, University of Konstanz, Konstanz, Germany
2 Matière et Systèmes Complexes, Université Paris-Diderot, Paris Cedex 13, France
3 UCA, INRA, UMR PIAF, 63000 Clermont-Ferrand, France

* rbastien@orn.mpg.de

Abstract

Plants regulate their shape and movements in accordance with their surrounding environment. This regulation occurs by a curving movement driven by differential growth. Recent studies has unraveled part of the mechanisms leading to differential growth though lateral polar auxin transport. However the real interplay between elongation, curvature variation, and accordingly the regulation process of growth distribution has not been really investigated so far. This issue is addressed in this study through gravitropic experiments on wheat coleoptiles, using a recently published kinematic approach, KimoRod. Here we show that median elongation is not affected by gravitropic perturbation. However kinematics studies reveal temporal oscillation of the median elongation rate. These oscillations propagate from the apex to the base during the movement with a characteristic velocity that is similar to auxin propagation in coleoptiles. The curvature variation exhibits a similar spatiotemporal pattern to the median elongation which reveals a nontrivial link between this two parameters and potential effect on perception and biomechanics of the tissue.

Introduction

In a fluctuating environment organisms must constantly regulate their posture [1]. Plants being usually clamped to the soil through their root system, their postural control is directly related to the movement they display during development. The local curvature of the plant organs is modified according to external and internal stimuli in order to change the spatial organization of the plant. These movements are driven by variation in growth between opposite side of the organ [2]. This asymmetry is currently interpreted using the Cholodny Went qualitative model. A modern point of view on the Cholodny-Went theory could be expressed as follow: Auxin, stimulating the growth of the cell, is redistributed asymmetrically inside the organ, according to the environmental stimuli (light or gravity for instance). This results in a difference in growth rate between opposite side of the organ and the bending of the organ [2,3]. Experimental works have given evidence to the validity of this theory and the biochemistry of this problem is now well known [4,5].

The first environmental factor that plants need to handle, in order to catch resources, is gravity [1,6]. Roots are oriented downwards, to reach nutriments, while

aerial organs are oriented upwards, to reach light. Studies on the kinematics of gravitropic movement have primarily focused on root, neglecting aerial organ [7–9]. But roots leaned inside the ground. The direction of the apical part only is regulated. The perception happens in the root cap and the curving is restricted to a small zone in the distal elongation zone [10]. On contrary aerial organ stand up in the air and the regulation of the posture is critical to reach specific spatial orientation. Here, both the perception and the active tropic curving is possible all along the elongation zone [6,10]. Experiments have focused on the first instants of the gravitropic reaction [11–13], neglecting the rest of the gravitropic movement. Others experiments have focused on the apical orientation [12–14], neglecting the influence of the basal curvature on the apical orientation [2,15]. This long-range effect of the basal curvature on the apical orientation prevents to relate directly observations of the apical orientation with the underlying dynamics of the plant organ.

Recently, we proposed to couple theoretical considerations with experimental kinematics [3,15]. A general behavior of the gravitropic movement has been observed among different species and organs and its control has been formalized in a unifying model called the AC model. Gravitropism was shown to be only driven by a unique number, B, "balance number", which expresses the ratio between two different perceptions: perception of gravity and proprioception. Proprioception is described as the ability of the plants to sense its own shape and responds accordingly, *i.e.* the organ can perceive its own curvature and modify its differential growth in order to remain straight [16]. If the number B is small, then proprioception tends to dominate the movement and the organ does not reach the vertical. On the contrary if B is large the organ oscillates around the vertical before the apical part is aligned with the gravity field. A simple relation between the final shape of the organ and the movement displayed has allowed to measure this number B through simple morphometric measurement.

This unifying model of gravitropism only accounts for a first order of the movement; If the previously described general pattern is observed in every plants and species studied in [3,15], experimental variations are often observed. In particular, plants tend to present a stronger regulation of the movement than predicted by the AC model. Many plants and organs does not overshoot the vertical in contradiction with prediction from morphometric measurement. The existence of a stronger and finer regulation is then expected. A joint regulation of longitudinal (median) elongation as well as of differential growth may be implied. As the movement is related to the available elongation, this regulation could not be understood properly without a clear and complete kinematics of the movement. Here we propose to study the kinematics of an organ in movements in order to identify new regulations that are linked to the postural control.

Experiments on wheat coleoptiles were conducted (Fig. 1). This choice have been influenced by the following factors : i. The organ never overshoot the vertical even for large B [3]. ii. Coleoptiles are mostly cylindrical organs without leaves or cotyledons. It is then easier to process image analysis than on an inflorescence, a hypocotyle or a stem where lateral organs could hide some part of the studied organ. iii. The organ is a germinative organ. It can be grown in the dark. Experiments can be conducted in the absence of light without modifying the normal physiological behavior of the organ. Thereby, phototropic effect can be avoided.

We recently developed a new tool to get the whole kinematics of an organ in movement, KimoRod [17]. This tool is based on the edge detection of the organ through a precise subpixellar algorithm. The median line is obtained with a very precise approximation by voronoi skeletonisation. From this median line, orientation and curvature is taken along the median line, by derivation on the curvilinear abscissa,
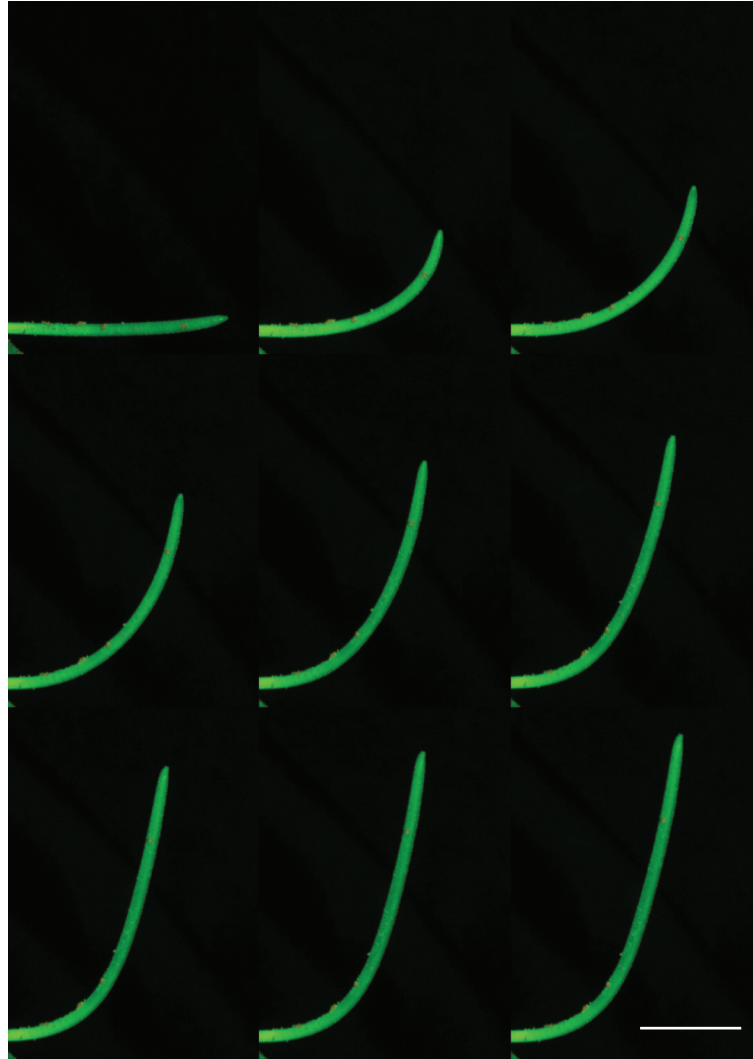
Fig 1. Straightening movement of a wheat coleoptile in the standard reading direction. 150 minutes between each frame. The white line accounts for 10 mm. The orange points on the coleoptile are fluorescent markers.

without interpolation. Finally, the elongation is obtained by a modified PIV algorithm (the Rod-PIV), where the sub-window of correlation is moved along the median line.

The use of an accurate and precise tool to measure organ growth and curvature opens the way to observe more details about the growth process. For instance, auxin is known to propagate from the apex to the base, at least during the first instants of the gravitropic response [4]. It has also been postulated that ultradian growth oscillation might be observed in relation to the dynamics of the growth process itself [18,19]. The spatial and and temporal resolution of KimoRod should be sufficient to observe those mechanisms.
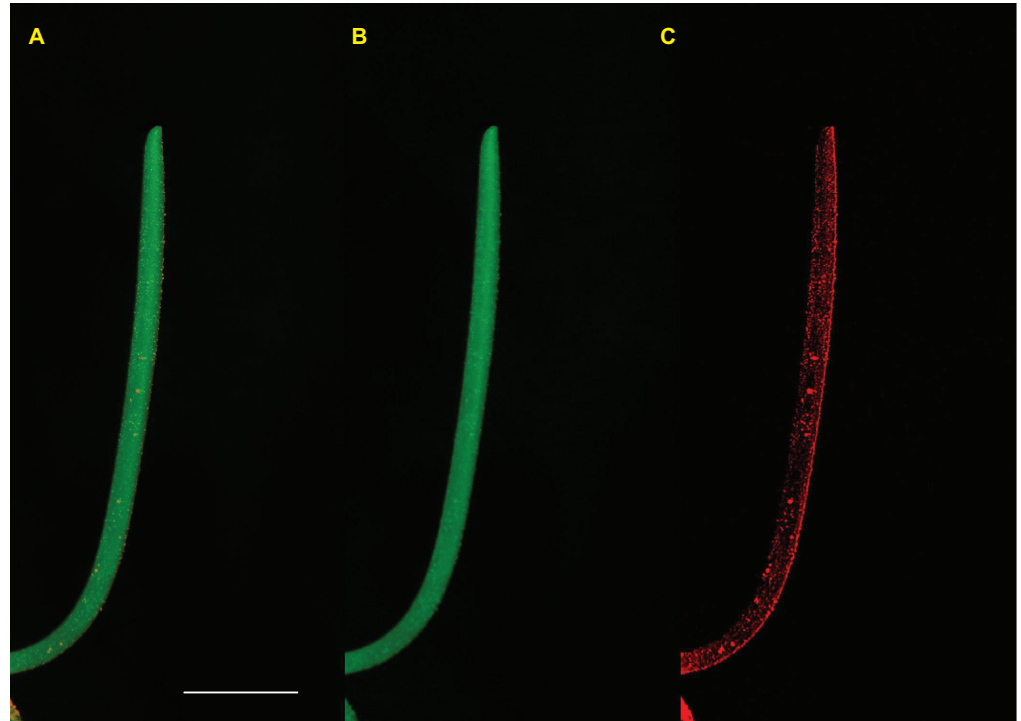
Fig 2. Picture of a coleoptile obtained from experiments before image analysis. The white line is 1cm. Pictures are taken in the dark with the flash light of the camera filtered in the green. A. The images taken directly from the camera. Color channels are separated: A. Green Channel. The coleoptile, white, appears green due to the green light. The markers do not modify the apparent shape of the object (no holes) because the orange fluorescent marker diffuse at the same time in the green and red channel. C. In the red channel, only the orange fluorescent markers are visible.

Materials and Methods

Plant Material

Seeds of wheat (Recital) are wetted during 6 hours. They are then positioned on cotton during 3 to 4 days at $25°C$ in the dark. The seeds are glued on a plastic tube filled with water and cotton at an angle of approximately $45°$, $\pi/4$,. This tilt of the seed should allow the coleoptile to start to grow upward, straight and vertical with minimal initial curvature. When the coleoptile is 10-20 mm long, it is placed in front of a camera (Olympus SP-550UZ or SP-560UZ) in the same conditions of temperature and darkness. Each coleoptile was sprinkled with non-toxic Orange fluorescent markers used as tracer particles for kinematics measurements (dry painting pigment Sennelier 648) (Fig. 2).

Time-lapse photography was taken every 15 minutes during 24 hours with the flash light of the camera filtered by a "safe" green light filter (Lee 139 Primary Green). Preliminary experiments showed that the intermittent green flashlight did not induce a phototropic movement (the coleoptile is not directed towards the flash) neither any greening. The markers did not alter elongation or bending of the organ.

Tropic experiment

The coleoptiles are splitted in two groups. The coleoptiles of the first group are tilted from the vertical with a $90°$ angle, $\pi/2$, from the vertical. Each coleoptile is tilted in the

plane made by the coleoptile with the seed. The seed is then placed downside the coleoptile. If the seed is in front of the camera some part of the coleoptile could be hidden by the coleoptile during the analysis. Also, the coleoptile could still be slightly curved in the plane made by the seed and the coleoptile, so if the coleoptile remains symmetrical about the image plane, all the movements are restricted inside this plane. 100

The coleoptiles from the second group are not tilted but remain vertical. This provide a control experiment where the organ is left without gravitropic perturbation. The coleoptile conserve the same orientation they had taken in the dark before the experiment, i.e. aligned with the direction of the gravity field.Pictures are taken in the direction perpendicular to the plane formed by the seed and the coleoptile. 105
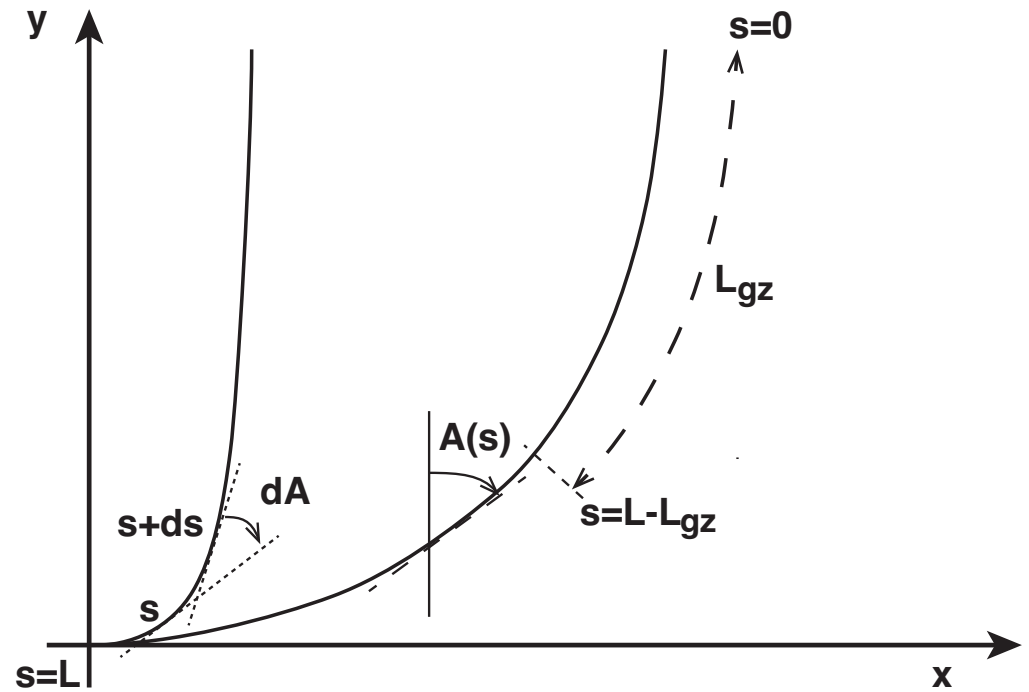
Fig 3. Geometric description of organ shape. The median line of an organ of total length L is in a plane defined by coordinates (x, y). The arc length s is defined along the median line, with $s = 0$ referring to the apex and $s = L(t)$ referring to the base. In an elongating organ, only the part inside the growth zone of length L_{gz} from the apex is able to curve (with $L_{gz} = L$ at early stages and $L_{gz} < L$ later on). $A(s, t)$ is the local orientation of the organ with respect to the vertical and $C(s, t)$ the local curvature. The two curves shown have the same apical angle $A(0, t) = 0$ but different shapes, so to specify the shape we need the form of $A(s, t)$ or $C(s, t)$ along the entire median line. Due to the symmetry of the system around the vertical axis, the angle $A(s, t)$ is a zenith angle, zero when the organ is vertical and upright. For simplicity, clockwise angles are considered as positive.

Kinematics 106

The kinematics of the movement is obtained with the use of the KimoRod software [17] (see Fig.3 for the geometry of the system). This software gives the median line of the organ and its curvilinear abscissa s from the apex to the base. The orientation from the vertical at each point along the organ is given for each picture $A(s, t)$. The curvature of 110

the organ $C(s,t)$ is then given by the derivative of the orientation along the median

$$C(s,t) = \frac{\partial C(s,t)}{\partial s} \tag{1}$$

The relative elongation growth rate of the median line (REGR) is obtained by a subcorrelation technique $\dot{E}(s,t)$. It is then possible to compute the material derivative of the curvature, the derivative following the materials point [2, 3, 6, 17]. According to the continuity equation, the material derivative (D/Dt) of the local variable $C(s,t)$ is calculated as

$$\frac{DC(s,t)}{Dt} = \frac{\partial C(s,t)}{\partial t} + \frac{\partial C(s,t)}{\partial s} \int_0^s dl \dot{E}(l,t) \tag{2}$$

Length of the growth zone, length of the curved zone and balance number B

As proposed in [15], the balance number B can be measured as the ratio between the length of the growth zone L_{gz} and the length of the curved zone length of the curved of the zone at steady state (when the organ reach an equlibrium shape), L_c

$$B = \frac{L_{gz}}{L_c} \tag{3}$$

On each experiment the relative elongation growth rate of the median line (REGR) as a function of the distance from the apex (s), $\dot{E}(s,t)$ is averaged over time

$$\dot{E}_a(s) = \frac{\int_{t_0}^{t_f} dt \dot{E}(s,t)}{\int_{t_0}^{t_f} dt} \tag{4}$$

where t_0 is the time at the beginning of the experiment and t_f the time at the end of the experiment. The length of the growth zone is then defined as the length from the apex that accounts for 98% of the total elongation. The length of the curved zone at steady state is obtained with the orientation at the final time time of experiments, t_f, measured on a curvilinear abscissa running from the first point inside the curved zone at the beginning of the experiment, $s_1 = L_g z$, to the apical part.

$$s' = (L(t_f) - s) - (L(t_0) - L_{gz}) \tag{5}$$

An exponential function, $A(s',t) = \exp^{-s'/L_c}$, is then fitted, and gives the characteristic length of the curved zone. B can then be obtained directly from eq. 3.

Periods of oscillation

As the signal could be really noisy, the time between non-successive peaks of elongation, respectively of the curvature variation, T_p has been measured. The period of the oscillation, T, is then given by the ratio of the time T_p by the number n of periods

$$T = \frac{T_p}{n} \tag{6}$$

Velocity of pulses propagation

The relative elongation growth rate of the median line, $\dot{E}(s,t)$, or the curvature variation, $DC(s,t)/Dt$, are represented on spatiotemporal kymograph. They are then thresholded to get the position of the maxima, respectively the minima, of the
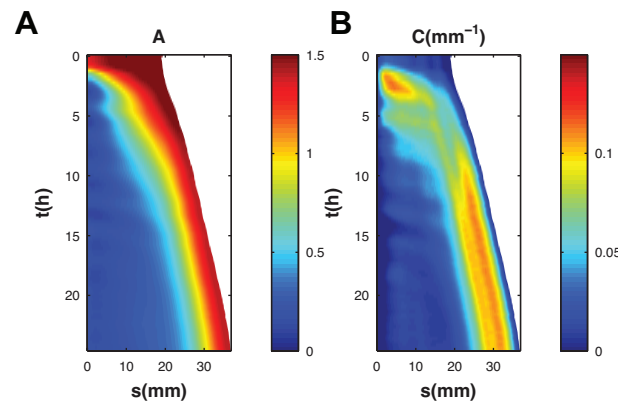
PLOS | SUBMISSION

oscillations. Each clouds of points is then fitted with a line, so that the position of the pulse along the median line, P(t), can be described by

$$P(t) = v_p t + t_p \tag{7}$$

where v_p is the velocity of propagation of the pulse from the apex to the base and t_p is the time of the pulse start.

Results

Curvature and orientation

Fig 4. Kinematics of gravitropic movement of a wheat coleoptile (from Fig. 1) shown as color maps plotting A. the orientation $A(s,t)$ and B. the curvature with respect to time t and curvilinear abscissa s (the arc length along the median measured from the apex $s = 0$ to the base of the organ $s = L$). As the coleoptile is elongating, the area covered is increasing with the time. The angle is measured from the vertical in radians. The curvature is measured in mm^{-1}.

The straightening movement of a wheat coleoptile is consistent with the generic pattern formalized in the AC model [15] and already observed in several other species of plants [15] (as observed on the kinematics of orientation and curvature Fig. 4). After being tilted the whole coleoptile curves. Then after 1 to 3 hours, as the apex reaches the vertical, the apical straightens as the curvature concentrates near the base. At the end the apical part of the coleoptile is mostly vertical, $A(s = 0) = 11° \pm 6°(.2 \pm .1)$, and rarely overshoot the vertical during the movement (less than 0.4% of all experiments). The length of convergence to the vertical is, $L_c = 5.0 \pm 0.2mm$.

Elongation

The typical patterns observed are represented on Fig.5. One coleoptile was vertical (Fig. 5.A-B), whereas the other was tilted from the vertical (Fig. 5.C-D). The relative elongation growth rate on the median line, $\dot{E}(t,s)$, is almost zero near the base of the coleoptile (Fig.5.A and C.). The elongation is limited to a zone near the apical part of the coleoptile. The length of the growth zone L_{gz} is not modified by the direction of the organ as $L_{gz} = 19.7 \pm 4.0mm$ for unperturbed vertical coleoptiles, and $L_{gz} = 19.3 \pm 3.0mm$ for tilted coleoptiles. However, inside this elongation zone, temporal oscillations of the median elongation appeared between values of approximately $\dot{E} \sim 1 \times 10^{-5}s^{-1} \sim 4 \times 10^{-2}h^{-1}$ and $\dot{E} \sim 2 \times 10^{-5}s^{-1} \sim 8 \times 10^{-2}h^{-1}$.
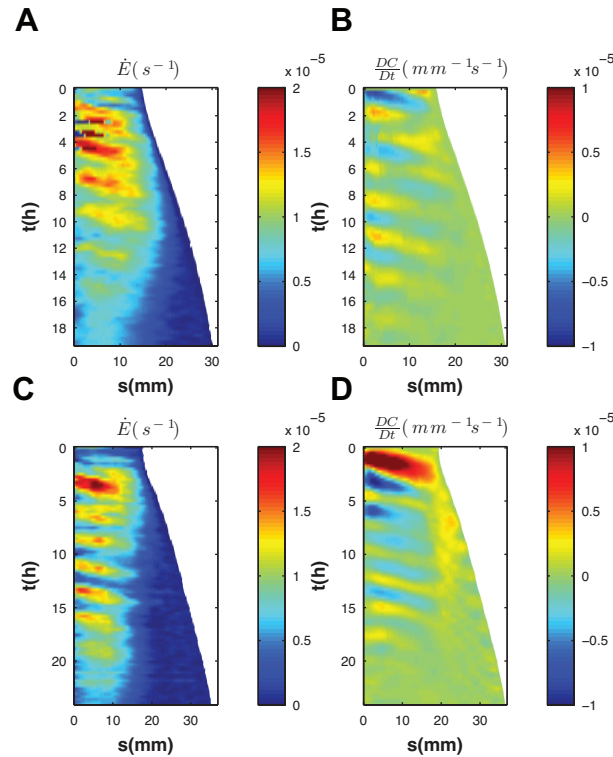
Fig 5. Relative Elongation Growth Rate $\dot{E}(s,t)$ **and curvature variation** $DC(s,t)/Dt$ **of two indivdual coleoptiles** A-B. untilted coleoptile, color maps plotting $\dot{E}(s,t)$ in s^{-1} (A) and the curvature variation in $mm^{-1}s^{-1}$ (B) with respect to time t and curvilinear abscissa s (the arc length along the median measured from the apex $s = 0$ to the base of the organ $s = L$). C-D the coleoptile has been tilted at 90° from the vertical.

The gravitropic perturbation did not modify these oscillations, as the temporal period is comparable $T_{\dot{E}} = 2.3 \pm 0.3h$ for unperturbed coleoptile and $T_{\dot{E}} = 2.1 \pm 0.3h$ for tilted coleoptiles.

This oscillatory behavior reveals a propagative mechanism of the elongation from the apex to the base. The apex starts to elongate before the more basal part. The velocity of propagation of the maximal elongation was comparable in all the experiments $v_p = 12.6 \pm 4.4mm.h^{-1}$ for the elongation (Figure 6).

A global view of the elongation along the organ can be obtained by the averaged elongation over time along the curvilinear abscissa $\dot{E}_a(s)$. This distribution has then been averaged on all experiments . The results are presented on Fig 7.A. There is no significant difference on the values of the elongation ($p = 0.24$), in both case most of the elongation is localized near the apex, and the elongation is maximal around $5mm$ from the apical part. The median elongation is independent of the direction of the organ.

Curvature variation and its relation with the elongation pattern

Temporal oscillations are also observed between curving phase in one direction (*e.g.* $DC/Dt > 0$) and in the other direction ($DC/Dt < 0$) (Fig. 5.B and D). This pattern is really similar to the pattern observed for the elongation (Fig. 5.A and C). Small oscillations are not a direct property of the gravitropic movement (Fig. 5.D) as they are also observed when the coleoptile remain vertical (Fig. 5.B). But the magnitude of the
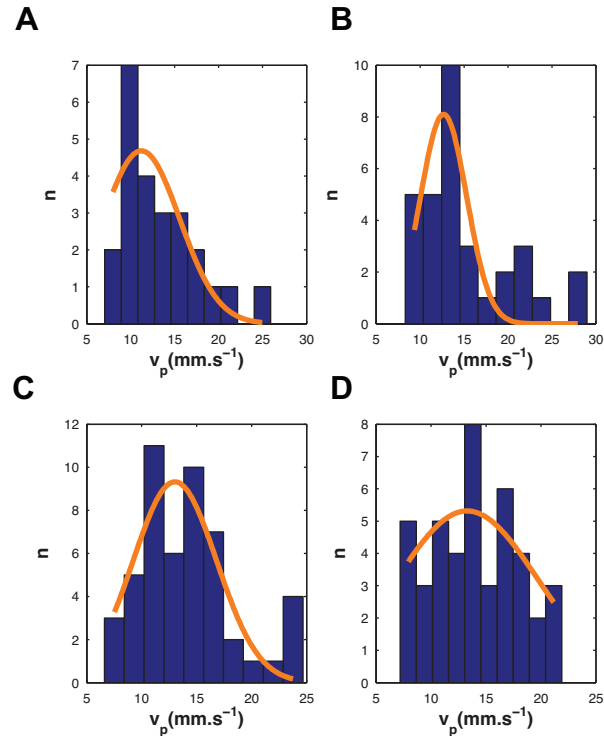
Fig 6. Histogram of the velocity of the propagation measured for the elongation $\dot{E}$ (A and B) and the curvature variation DC/Dt (C and D) for non-tilted coleoptiles (A and C) and tilted ones (B and D) The Orange line is the gaussian fit of the histogram. A. $v_p = 11.2 \pm 4.3 mm.h^{-1}$, B. $v_p = 12.7 \pm 2.6 mm.h^{-1}$, C. $v_p = 13.0 \pm 3.7 mm.h^{-1}$ and D. $v_p = 12.6 \pm 6.0 mm.h^{-1}$

oscillation is smaller than in the tilted case. The averaged value of the absolute variation of curvature is indeed different when the coleoptile is tilted or curved ($p \sim 0$) (Fig.7.B). During the first hours, the tilted coleoptile display a strong curvature variation all along the stem. This is followed by a strong curvature variation in the other direction, which can be associated to a straightening process. The base is still curving (note that in the non-elongating part there is no curvature variation). At the end of the straightening movement, the amplitude of the oscillation become similar to those observed in the untilted case.

The periods of the oscillations are comparable ($T_{DC} = 2.3 \pm 0.3h$) for untilted coleoptile and for tilted coleoptile ($T_{DC} = 2.3 \pm 0.2h$) (Fig. 6). For each individual coleoptile, one can see a strong correlation between the frequencies of the oscillations of the REGR and of the curvature variation (Fig. 8). Furthermore the curvature variation propagates from the apex to the base. The velocity of propagation was comparable in all the experiments (Fig. 6). For tilted coleoptiles, the correlation of the median elongation rate pattern with the material curvature variation pattern is also mostly negative (Fig. 8.D). This negative correlation implies that the coleoptile tends to straighten when the elongation rate is maximal whereas the coleoptile curves when the elongation rate is small (Fig. 5 and 8). In the case of untilted coleotpiles, the low values of the curvature variation prevents to see this correlation (Fig. 8.C), but this correlation remains visible on the correlation of the oscillatory periods (Fig. 8.A).
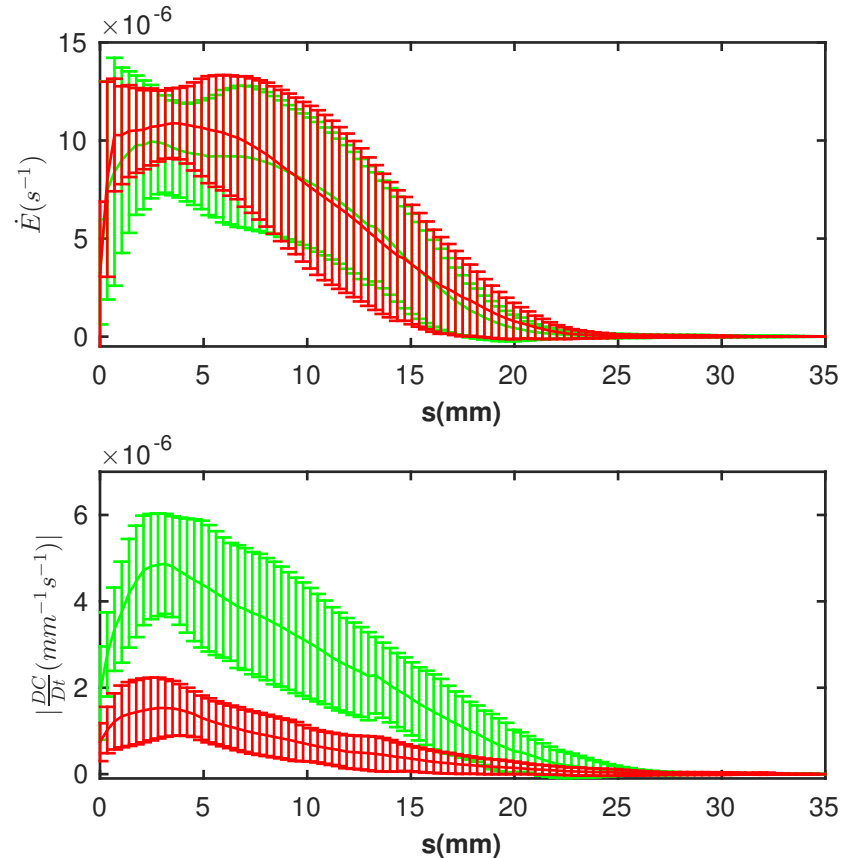
Fig 7. Averaged Elongation (A) and the absolute Curvature variation (B) along the curvilinear abscissa from the apex to the base during the first 12h hours after stimulation. In red, the coleoptile is not tilted and vertical, in green the coleoptile is tilted 90° from the vertical. The standard deviation accounts for the difference between experiments.

Discussion

With an averaged B on all of the experiments of 3.9 ± 0.6, and according to the AC model [15], the coleoptile is expected to overshoot the vertical in most of the experiments. This overshoot is rarely observed, less than 0.4% of all experiments. A more advanced regulation is then likely to be involved, in addition to the AC core model.

The pattern of relative elongation growth rate on the median line remains unchanged during gravitropic perturbation. Even if the local auxin flux is redistributed axially, the longitudinal redistribution of the local auxin flux is not modified. Gravitropism does not redistribute the elongation to increase the curvature of the most tilted part. Tropic curvature can only be achieved through the local transverse distribution of the elongation at each point along the stem.

This study reveals an oscillatory behavior of the relative elongation growth rate on the median elongation (REGR) of the wheat coleoptile, $\dot{E}(s,t)$. Tobias Baskin [19] has discussed the existence of ultradian oscillatory mechanism of growth but, these oscillatory mechanisms have only been rarely reported, *e.g.* during the nutation of sunflower hypocotyls [20]. However, this measurements are not realized on the median line but on opposite sides of the organ. Oscillation of differential growth are expected to account for the observed oscillatory movement [21]. The variation of the relative
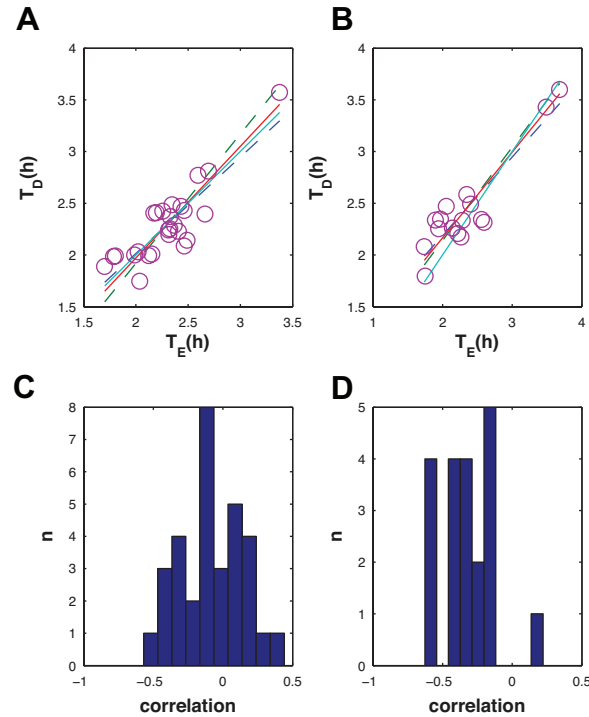
Fig 8. A. and B. Correlation of the oscillatory period of the elongation in abscissa and of the curvature variation in ordinate for untilted coleoptiles (A) and tilted ones (B). A. The correlation is significant ($p - value \sim 10^{-9}$) and the slope is near from 1 ($p - value \sim .96$), furthermore the slope cannot be distinguished from 1 ($p - value \sim .35$). B. The correlation is still significant ($p - value \sim 10^{-9}$) and the slope is near from 1 ($p - value \sim .85$). C. and D. Correlation of the pattern between the curvature variation and the elongation. The correlation is made on the whole experiment but limited to a length from the apex equivalent to the initial length. C. untilted coleoptiles and D. tilted ones.

elongation growth rate on the median line was not discussed. Tip growth oscillations have also been measured on pollen tube due to pH variation [22] or calcium activity [23]. But the pollen tube is a unique cell displaying tip growth and the characteristic scale of the oscillations, less than a minute on $10um$, are really different from the oscillations observed on the wheat coleoptile, about two hours on $2cm$.

By tracking the maxima of the elongation, propagation from the apex to the base is revealed. This could be related to the propagation of auxin as the average velocity of propagation of Auxin in coleoptile ($12mm.h^{-1}$ according to [24–26]) is compatible with our own observations ($v_p = 12.6 \pm 4.4mm.h^{-1}$). Auxin is also known to play a major role as a growth factor so it is a reasonable candidate to explain the propagation from the apex to the base of the elongation.

However this remain insufficient to explain the oscillatory behavior of the elongation and the associated characteristic time, $2.2h$ between 2 pulses. Oscillatory pulses of auxin in a coleoptile have been measured [25, 27, 28], but the characteristic time between 2 pulses is around 25-30 minutes, 4 times faster than our observation. The dynamics of auxin is then insufficient to account for the oscillations described in this study.

Similar oscillations of the curvature variation have also been revealed. this could be related to experiment that tracked the apical part of coleoptile. An oscillatory movement was revealed during gravitropic movement [13]. No conclusive mechanism

were found as the kinematics only focused on the movement of the apical part of the coleoptile. Our current observation provides a simple basis to this behavior. Global measurements, such as the apical orientation, must be taken carefully as they can hide more general local mechanisms such as oscillatory behavior and non-trivial relation between curvature variation and elongation (see [17] for a discussion on the limits of tracking the apical part of the organ only).

The characteristics of the oscillations of the curvature variation are similar to those of the relative elongation growth rate on the median line. This relation is not trivial indeed. The curvature variation can be expressed as a function of the elongation rate [3]

$$\frac{DC(s,t)R}{Dt} \sim \dot{E}(s,t)\Delta(s,t) \tag{8}$$

where $\Delta(s,t)$ accounts for the distribution of the differential growth on each side of the coleoptile. While $\Delta(s,t)$ can be measured as the ratio between the variation of curvature and the elongation rate

$$\Delta(s,t) \sim \dot{E}(s,t)^{-1}\frac{DC(s,t)R}{Dt} \tag{9}$$

this measure tends to be very noisy. However the regulation of the gravitropic movement and the mechanism under the non-trivial link between elongation and curvature variation can be discussed from the measurement of the elongation rate $\dot{E}(s,t)$ and the curvature variation $\frac{DC(s,t)}{Dt}$. As no global shrinking of the organ is expected, $\dot{E}(s,t)$ is always positive. The local elongation rate can only modulate the amplitude of the curvature rate but not its sign, the direction in which the organ is curved can not be changed. As the curvature variation goes in different way depending on the elongation oscillation, the differential growth term $\Delta(s,t)$ must be correlated to the variation of $\dot{E}(s,t)$.

To understand this non trivial correlation, different hypotheses can be postulated. For instance, the general model of gravitropism has been described to be dependent on two different parameters acting in an opposite way so that a dynamical equilibrium can be reached [15]. Graviception tends to curve the coleoptile in order the stem to be vertical whereas proprioception tends to straighten the stem. Depending on the value of the elongation rate, one perception process could dominate the others.

Recent studies on the acto-myosin complex can provide a molecular and mechanistic point of view on this question. It is now well known that the graviception is directly related to the actin cytoskeleton [5, 29, 30]. The disruption of the actin cytoskeleton by the use of drugs could enhance the response to the gravity, which would have then a direct effect on the value of the graviceptive term β. A similar and opposite effect have recently been revealed on the straightening of Arabidopsis inflorescence [31, 32]. A straightening deficiency is observed when the myosin complex is disrupted. The influence of the proprioceptive term, γ, is then expected to be reduced. Finally the configuration of the actin cytoskeleton is directly linked to the available auxin [28, 33]. This is amplified by an active feedback where the transport of the auxin is enhanced by the actin cytoskeleton. This would provide a simple explanation of the observed relation between curvature variation and elongation rate, where graviception and proprioception can dominate different part of the dynamics due to the opposite effects of the actin-myosin complex and its relation with auxin.

PLOS | SUBMISSION

Acknowledgments

281

References

1. Moulia B, Coutand C, Lenne C. Posture control and skeletal mechanical acclimation in terrestrial plants: Implications for mechanical modeling of plant architecture. American Journal of Botany. 2006;93(10):1477–1489.

2. Silk WK. Quantitative descriptions of development. Annual Review of Plant Physiology. 1984;35:479–518.

3. Bastien R, Douady S, Moulia B. A unifying modeling of plant shoot gravitropism with an explicit account of the effects of growth. Frontiers in plant science. 2014;5:136.

4. Philippar K, Fuchs I, Lüthen H, Hoth S, Bauer CS, Haga K, et al. Auxin-induced K+ channel expression represents an essential step in coleoptile growth and gravitropism. Proceedings of the National Academy of Sciences of the United States of America. 1999;96(21):12186–12191.

5. Morita MT. Directional gravity sensing in gravitropism. Annual review of plant biology. 2010;61:705–720.

6. Moulia B, Fournier M. The power and control of gravitropic movements in plants: a biomechanical and systems biology view. J Exp Bot. 2009;60(2):461–486.

7. Walter A, Spies H, Terjung S, Kusters R, Kirchgessner N, Schurr U. Spatio-temporal dynamics of expansion growth in roots: automatic quantification of diurnal course and temperature response by digital image sequence processing. J Exp Bot. 2002;53(369):689–698.

8. Basu P, Pal A, Lynch JP, Brown KM. A Novel Image-Analysis Technique for Kinematic Study of Growth and Curvature. Plant Physiol. 2007;145(2):305–316.

9. Chavarria-Krauser A, Nagel KA, Palme K, Schurr U, Walter A, Scharr H. Spatio-temporal quantification of differential growth processes in root growth zones based on a novel combination of image sequence processing and refined concepts describing curvature production. New Phytologist. 2008;177(3):811–821.

10. Bastien R, Douady S, Moulia B. A unified model of shoot tropism in plants: photo-, gravi-and propio-ception. PLoS Comput Biol. 2015;11(2):e1004037.

11. Cosgrove DJ. Rapid, bilateral changes in growth rate and curvature during gravitropism of cucumber hypocotyls: implications for mechanism of growth control. Plant Cell Environ. 1990;13(3):227–34.

12. Iino M, Tarui Y, Uematsu C. Gravitropism of maize and rice caleoptiles: Dependence on the stimulation angle. Plant Cell and Environment. 1996;19(10):1160–1168.

13. Tarui Y, Iino M. Gravitropism of oat and wheat coleoptiles: Dependence on the stimulation angle and involvement of autotropic straightening. Plant and Cell Physiology. 1997;38(12):1346–1353.

14. Galland P. Tropisms of Avena coleoptiles: sine law for gravitropism, exponential law for photogravitropic equilibrium. Planta. 2002;215(5):779–84.

PLOS | SUBMISSION

15. Bastien R, Bohr T, Moulia B, Douady S. Unifying model of shoot gravitropism reveals proprioception as a central feature of posture control in plants. Proceedings of the National Academy of Sciences. 2013;110(2):755–760.

16. Hamant O, Moulia B. How do plants read their own shapes? New Phytologist. 2016;.

17. Bastien R, Legland D, Martin M, Fregosi L, Peaucelle A, Douady S, et al. KymoRod: a method for automated kinematic analysis of rod-shaped plant organs. The Plant Journal. 2016;.

18. Zajkaczkowski S, Wodzicki T, Romberger J. Auxin waves and plant morphogenesis. In: Hormonal Regulation of Development II. Springer; 1984. p. 244–262.

19. Baskin TI. Ultradian Growth Oscillations in Organs: Physiological Signal or Noise? In: Mancuso S SS, editor. Rythms in Plants. Springer; 2006. .

20. Berg AR, Peacock K. GROWTH-PATTERNS IN NUTATING AND NONNUTATING SUNFLOWER (HELIANTHUS-ANNUUS) HYPOCOTYLS. American Journal of Botany. 1992;79(1):77–85.

21. Bastien R, Meroz Y. The Kinematics of Plant Nutation Reveals a Simple Relation Between Curvature and the Orientation of Differential Growth. accepted for publication in Plos Computational Biology. 2016;.

22. Monshausen GB, Bibikova TN, Messerli MA, Shi C, Gilroy S. Oscillations in extracellular pH and reactive oxygen species modulate tip growth of Arabidopsis root hairs. Proceedings of the National Academy of Sciences. 2007;104(52):20996–21001.

23. Monshausen GB, Messerli MA, Gilroy S. Imaging of the Yellow Cameleon 3.6 Indicator Reveals That Elevations in Cytosolic Ca2+ Follow Oscillating Increases in Growth in Root Hairs of Arabidopsis. Plant Physiol. 2008;147(4):1690–1698.

24. Shen-Miller J. Rhythmicity in the basipetal transport of indoleacetic acid through coleoptiles; 1972. Division of Biological and Medical Research annual report, 1972 United States System Entry Date: 06/03/2001 Source: NSA-28-015102; TIC (Technical Information Center) Language: English.

25. Shen-Miller J. Rhythmic Differences in the Basipetal Movement of Indoleacetic Acid between Separated Upper and Lower Halves of Geotropically Stimulated Corn Coleoptiles. Plant Physiol. 1973;52(2):166–170.

26. Kramer EM, Rutschow HL, Mabie SS. AuxV: a database of auxin transport velocities. Trends in plant science. 2011;16(9):461–463.

27. Goldsmith MHM. Movement of pulses of labeled auxin in corn coleoptiles. Plant physiology. 1967;42(2):258–263.

28. Nick P. Probing the actin-auxin oscillator. Plant signaling & behavior. 2010;5(2):94–98.

29. Yamamoto K, Kiss JZ. Disruption of the Actin Cytoskeleton Results in the Promotion of Gravitropism in Inflorescence Stems and Hypocotyls of Arabidopsis. Plant Physiol. 2002;128(2):669–681.

PLOS | **SUBMISSION**

30. Hou G, Mohamalawari DR, Blancaflor EB. Enhanced Gravitropism of Roots with a Disrupted Cap Actin Cytoskeleton. Plant Physiol. 2003;131(3):1360–1373.

31. Okamoto K, Ueda H, Shimada T, Tamura K, Kato T, Tasaka M, et al. Regulation of organ straightening and plant posture by an actin–myosin XI cytoskeleton. Nature plants. 2015;1(4).

32. Ueda H, Tamura K, Hara-Nishimura I. Functions of plant-specific myosin XI: from intracellular motility to plant postures. Current opinion in plant biology. 2015;28:30–38.

33. Nick P, Han MJ, An G. Auxin stimulates its own transport by shaping actin filaments. Plant Physiology. 2009;151(1):155–167.